Multi-branch shell models of two-dimensional turbulence exhibit dual energy-enstrophy cascades

Flavio Tuteri,[1,*] Sergio Chibbaro,[2] and Alexandros Alexakis[1]
[1] *Laboratoire de Physique de l'École normale supérieure, ENS, Université PSL, CNRS, Sorbonne Université, Université Paris Cité, F-75005 Paris, France*
[2] *Université Paris-Saclay, CNRS, UMR 9015, LISN, F-91405 Orsay Cedex, France*

(Received 13 March 2026; accepted 21 July 2026; published 11 August 2026)

Classical shell models of turbulence do not display dual cascade—inverse for energy and direct for enstrophy—because they fail to reproduce the right thermal spectra. We propose here a multi-branch shell model, including a geometry hierarchically organized across scales, in order to overcome this limitation. For this model, we demonstrate numerically both the agreement of the thermal spectra with those of two-dimensional fluid equations and the emergence of a statistically stationary dual cascade. This construction also allows us to study local transfers and to investigate both self-similarity and non-Gaussianity.

DOI: 10.1103/5bxw-xd8z

I. INTRODUCTION

Reduced models of nonlinear chaotic systems with many degrees of freedom and interactions play a fundamental role in theoretical development [1]. They provide valuable laboratories for testing ideas, provided that these reduced systems are able to capture, at least qualitatively, the phenomenology of the underlying physical systems. For Navier-Stokes systems, shell models, based on Fourier shell averaging, have been used to develop and test theories of turbulence [2–5]. Shell models of three-dimensional turbulence successfully reproduce the forward energy and helicity cascade as well as the presence of intermittency.

However, the dual cascade of energy and enstrophy of two-dimensional turbulence has been difficult to reproduce. In two dimensions, enstrophy (the squared curl of the velocity) cascades to small scales, while energy cascades inversely to large scales, leading to a k^{-3} spectrum for scales smaller than the forcing scale and a $k^{-5/3}$ spectrum for scales larger than the forcing scale [6]. The failure of shell models to reproduce these cascade processes in two dimensions is linked to the more serious inability to reproduce the correct equilibrium states. These are states achieved in finite wave number systems in the absence of any forcing and dissipation that lead, under certain conditions, to equipartition of conserved quantities among all degrees of freedom. In the (truncated) two-dimensional Navier-Stokes equation the equilibrium states lead to a k^1 spectrum for the equipartition of energy and a k^{-1} spectrum for the equipartition of enstrophy [7–9]. Classical shell models with one dynamical variable per shell, however, result in equivalent k^{-1} and k^{-3} spectra for the equipartition of energy and enstrophy, respectively. The fact that the enstrophy equipartition spectrum coincides with the forward cascade of the enstrophy spectrum prevents the dual cascade of energy and enstrophy from manifesting [10]. As an alternative, to achieve an inverse cascade in shell models that mimics the dual cascade scenario of two-dimensional turbulence, the conservation of a pseudoenstrophy that has physical dimensions of velocity squared times $k^{2\alpha}$, with

*Contact author: flavio.tuteri@phys.ens.psl.eu

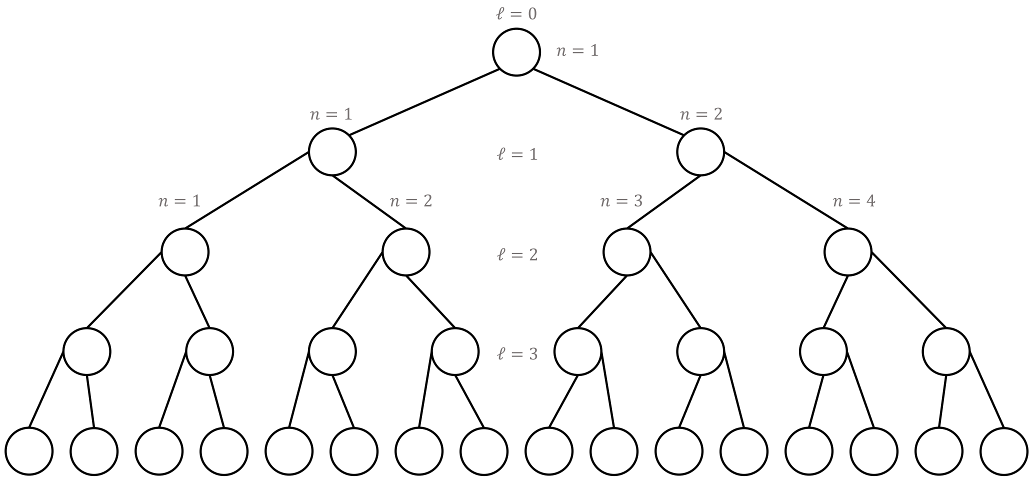

FIG. 1. Schematic representation of the dyadic shell model topology. Each level ℓ corresponds to a shell with characteristic wave number $k_\ell = \lambda^\ell$, while the index n labels spatial substructures of the same characteristic length scale.

$\alpha < 1$, is imposed [11–13]. This alternative does, indeed, reproduce the dual cascade scenario, but with spectra that do not coincide with the two-dimensional turbulence predictions.

This difficulty can be overcome for a new class of models with a hierarchical organization of spatial degrees of freedom across scales. Such shell models were introduced long ago [14–17] but have recently been reexamined [18,19]. These models predict the correct equilibrium spectra, and the direct cascade of enstrophy is possible, as shown in [16]. However, no demonstration of the dual cascade in two-dimensional turbulence has been given so far.

In Sec. III we show that these models can reproduce the dual cascade scenario with a forward cascade of enstrophy and an inverse cascade of energy. In the Appendix we also provide a discussion of the computational scalability of the model.

II. MODEL

We recall that a shell model is heuristically a reduction of the degrees of freedom in the Navier-Stokes equations, obtained through a spherical coarse graining in Fourier space that retains only quasilocal triadic interactions [4,20]. Nonetheless, geometry plays a fundamental role in turbulence, and therefore, the introduction of additional spatial degrees of freedom was previously proposed [14–19]. Compared with previous proposals, the present construction combines a hierarchical organization of space across scales with a nonlinear term adapted to the corresponding volume-weighted invariants. Indeed, here the nonlinear coupling has to be compatible not only with the shell-to-shell triadic structure but also with the volume weights associated with the spatial interpretation of the tree.

A. Definition

We introduce a shell model framework defined on a p-adic tree topology. The state is specified by complex dynamical variables $u_{\ell,n}$ associated with the nodes

$$(\ell, n), \quad \ell \in \{0, \dots, L\},\ n \in \{1, \dots, p^\ell\}. \tag{1}$$

See Fig. 1 for the case with $p = 2$. The level index ℓ plays the role of the scale index and is associated with the wave number $k_\ell = \lambda^\ell$, with intershell ratio $\lambda > 1$. For fixed ℓ, the index n labels spatial substructures at the corresponding characteristic length. With this interpretation, global observables are defined as volume-weighted sums of local densities. In particular, the total energy and enstrophy read

$$E = \frac{1}{2}\sum_{\ell=0}^{L} {k_\ell}^{-D} \sum_{n=1}^{p^\ell} |u_{\ell,n}|^2, \quad Z = \frac{1}{2}\sum_{\ell=0}^{L} {k_\ell}^{2-D} \sum_{n=1}^{p^\ell} |u_{\ell,n}|^2, \tag{2}$$

where D denotes the effective spatial dimension. Note that the factor ${k_\ell}^{-D}$ expresses the D-dimensional volume of the structure at scale ℓ. Accordingly, the energy spectrum E_ℓ is defined as

$$E_\ell = \frac{1}{2}{k_\ell}^{-D} \sum_{n=1}^{p^\ell} |u_{\ell,n}|^2. \tag{3}$$

Interactions between nodes have to be compatible with genealogy. Each node (ℓ, n), except the root (0,1), has a single parent $(\ell - 1, \lceil n/p \rceil)$, where $\lceil x \rceil = \min\{m \in \mathbb{Z} \mid m \geqslant x\}$ is the ceiling. Each node (ℓ, n), except the leaves (L, n), has p children, namely, $(\ell + 1, p(n-1)+1), \ldots, (\ell + 1, pn)$. The dynamics on this topology is defined by

$$\left[\frac{d}{dt} + \nu {k_\ell}^{2n_\nu} + \alpha {k_\ell}^{-2n_\alpha}\right] u_{\ell,n} = i N_{\ell,n}[u] + f_{\ell,n}, \tag{4}$$

where ν and n_ν fix the hyperviscous dissipation, α and n_α define the hypoviscous drag, $f_{\ell,n}$ is the forcing, and $N_{\ell,n}$ is the nonlinear coupling. Our model generalizes the Sabra coupling [21] by equally distributing admissible triads along genealogical branches:

$$N_{\ell,n} = k_\ell \left[a\,\lambda \,\frac{1}{p}\sum_{h=0}^{p-1}\left({u_{\ell+1,pn-h}}^* \,\frac{1}{p}\sum_{m=0}^{p-1} u_{\ell+2,p(pn-h)-m}\right) + b {u_{\ell-1,\lceil n/p \rceil}}^* \,\frac{1}{p}\sum_{m=0}^{p-1} u_{\ell+1,pn-m} \right.$$
$$\left. - c\,\lambda^{-1} u_{\ell-2,\lceil n/p^2 \rceil} u_{\ell-1,\lceil n/p \rceil} \right], \tag{5}$$

supplemented by the boundary conditions $u_{-2,\bullet} = u_{-1,\bullet} = 0 = u_{L+1,\bullet} = u_{L+2,\bullet}$. Homogeneous solutions, i.e., constant in n, correspond to the classical single-branch model. The inviscid and unforced dynamics conserves the total energy provided that

$$a + b + c = 0, \tag{6}$$

together with the condition

$$D^{-1} = \log_p \lambda. \tag{7}$$

Relation (7) expresses the geometric consistency of the cascade: The branching number p equals the volume contraction between successive scales. Requiring, in addition, the conservation of enstrophy leads to the further constraint

$$a + \lambda^2 b + \lambda^4 c = 0. \tag{8}$$

The local energy transfer from $(\ell - 1, \lceil n/p \rceil)$ to (ℓ, n) is defined as the rate of change of the energy contained in (ℓ, n) and in all descendant nodes:

$$\Pi^{e}{}_{\ell,n} = \mathrm{Im}\left[\sum_{j=\ell}^{L} {k_j}^{-D} \sum_{m=p^{j-\ell}(n-1)+1}^{p^{j-\ell} n} u_{j,m} N_{j,m}[u]^*\right] \tag{9}$$

$$= {k_\ell}^{1-D}\,\mathrm{Im}\left[-a\,u_{\ell-1,\lceil n/p\rceil}u_{\ell,n}\,\frac{1}{p}\sum_{m=0}^{p-1}{u_{\ell+1,pn-m}}^* + c\,\lambda^{-1}\,u_{\ell-2,\lceil n/p^2\rceil}u_{\ell-1,\lceil n/p\rceil}{u_{\ell,n}}^*\right]. \quad (10)$$

Expression (10) is a direct consequence of energy conservation (6). Analogously, we derive the local enstrophy flux:

$${\Pi^z}_{\ell,n} = \mathrm{Im}\left[\sum_{j=\ell}^{L}{k_j}^{2-D}\sum_{m=p^{j-\ell}(n-1)+1}^{p^{j-\ell}n}u_{j,m}N_{j,m}[u]^*\right] \quad (11)$$

$$= {k_\ell}^{3-D}\,\mathrm{Im}\left[-\lambda^{-2}a\,u_{\ell-1,\lceil n/p\rceil}u_{\ell,n}\,\frac{1}{p}\sum_{m=0}^{p-1}{u_{\ell+1,pn-m}}^* + c\,\lambda^{-1}\,u_{\ell-2,\lceil n/p^2\rceil}u_{\ell-1,\lceil n/p\rceil}{u_{\ell,n}}^*\right]. \quad (12)$$

In a statistically stationary regime, the system may sustain a dual cascade characterized by constant mean fluxes across scales,

$$\langle{\Pi^e}_{\ell,n}\rangle_{n,t} = \epsilon_e \quad \text{for } k_\ell \ll k_f, \quad \langle{\Pi^z}_{\ell,n}\rangle_{n,t} = \epsilon_z \quad \text{for } k_\ell \gg k_f, \quad (13)$$

where k_f denotes the forcing wave number and ϵ_e and ϵ_z are the mean energy and enstrophy injection rates, respectively.

B. Equilibrium

To assess the possibility of a dual cascade, direct for enstrophy and inverse for energy, we analyze the corresponding Gibbs equilibrium states. In our interpretation, when a thermal state exists with the same spectral scaling as a cascade solution, the nonlinear dynamics can satisfy the spectral constraint through local thermalization without sustaining a persistent intershell transfer. As a result, the mean flux across scales vanishes. For our model, the inviscid and unforced dynamics conserves two quadratic quantities, so that the corresponding Gibbs equilibrium measure is

$$P[u] \propto \exp[-\beta E - \gamma Z] = \exp\left\{-\frac{1}{2}\sum_{\ell=0}^{L}\left[\left(\beta {k_\ell}^{-D} + \gamma k_\ell^{2-D}\right)\sum_{n=1}^{p^\ell}|u_{\ell,n}|^2\right]\right\}, \quad (14)$$

with $\beta, \gamma > 0$. Under this measure,

$$E_\ell = \frac{1}{k_\ell^D}\sum_n\langle|u_{\ell,n}|^2\rangle_P = \langle|u_{\ell,n}|^2\rangle_P = \frac{{k_\ell}^D}{\beta + \gamma k_\ell^2}, \quad (15)$$

where in the second equality we have used the fact that the mode energy is independent of n, together with Eq. (7). Extreme cases for the thermal spectrum are

$$E_\ell \propto {k_\ell}^D, \quad (16)$$

corresponding to equipartition of energy, and

$$E_\ell \propto {k_\ell}^{D-2}, \quad (17)$$

corresponding to equipartition of enstrophy. For $D = 2$, the present model yields thermal spectra $E_\ell \propto {k_\ell}^2$ and $E_\ell \propto {k_\ell}^0$, consistent with those of two-dimensional Navier-Stokes systems once the shell-averaging factor is properly taken into account. In Fig. 2 we numerically verify prediction (16) and (17) for the 2-adic model with $D = 2$. In these runs, simulations of model (4) were performed with no forcing and no dissipation and initial conditions that had most of the energy in the small wave numbers (left panel) and most of the energy in the large wave numbers (right panel). At late times the thermal energy spectra were reproduced.

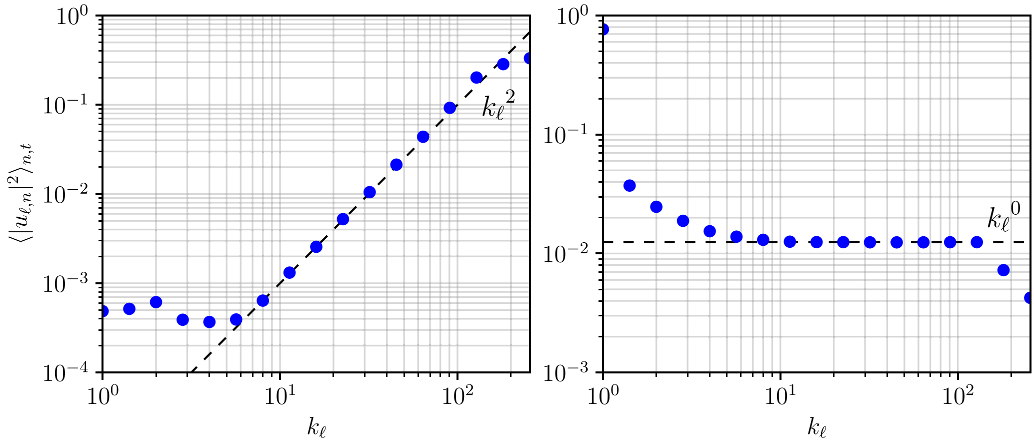

FIG. 2. Thermal spectra obtained from the inviscid and unforced dynamics for $D = 2$. At equilibrium, the scaling (15) is recovered. Left: initial condition with energy concentrated at small scales. Right: initial condition with energy concentrated at large scales.

III. RESULTS

We report the results of numerical simulations evolving (4) with 2-adic branching, with intershell ratio $\lambda = \sqrt{2}$ ($\Leftrightarrow D = 2$), hyperviscosity $\nu = 10^{-12}$ with $n_\nu = 2$, large-scale drag $\alpha = 0.5$ with $n_\alpha = 2$, and forcing injecting energy in shells $\ell_f = 11$–13 over a total of 25 shells. Figure 3 shows the mean energy spectrum (top) and the corresponding mean fluxes of energy and enstrophy (bottom). The spectrum exhibits a ${k_\ell}^{-2/3}$ scaling at scales larger than the forcing band and a ${k_\ell}^{-2}$ scaling at smaller scales. These scalings are consistent with an inverse energy cascade and a direct enstrophy cascade, respectively, as confirmed by the behavior of the mean fluxes in the bottom panel.

To investigate the inverse cascade inertial range, we analyze the statistics of the local energy flux. Figure 4 shows the probability density functions of the local energy flux ${\Pi^e}_{\ell,n}$ at different scales ℓ. Assuming spatial ergodicity, different values of n are interpreted as independent samplings of the same random variable. Because the number of nodes at level ℓ scales as 2^ℓ, smaller values of ℓ provide fewer statistical samples. The higher noise observed for probability density functions at small ℓ is therefore a finite-sample effect rather than a dynamical feature. The distributions are rescaled by their maxima, and the collapse is observed, indicating self-similarity despite strongly non-Gaussian statistics, as observed for the local energy flux in direct numerical simulations of two-dimensional Navier-Stokes turbulence [22,23]. The inset shows the scaling exponents of the local energy-flux structure functions. The error analysis follows the procedure proposed in [24]. The measured exponents follow the dimensional prediction based on self-similarity.

To test the robustness of the turbulent inertial ranges, we performed additional simulations with forcing applied either at large scales (Fig. 5) or at small scales (Fig. 6). This separates the two transfer processes and allows us to observe the corresponding inertial ranges over more than one decade in scale.

IV. CONCLUSIONS

We studied a multi-branch shell model with a hierarchical organization of spatial degrees of freedom across scales. Within this class of models, dimensional analysis allows the identification of a configuration whose thermal equilibrium reproduces the scaling expected for two-dimensional fluids.

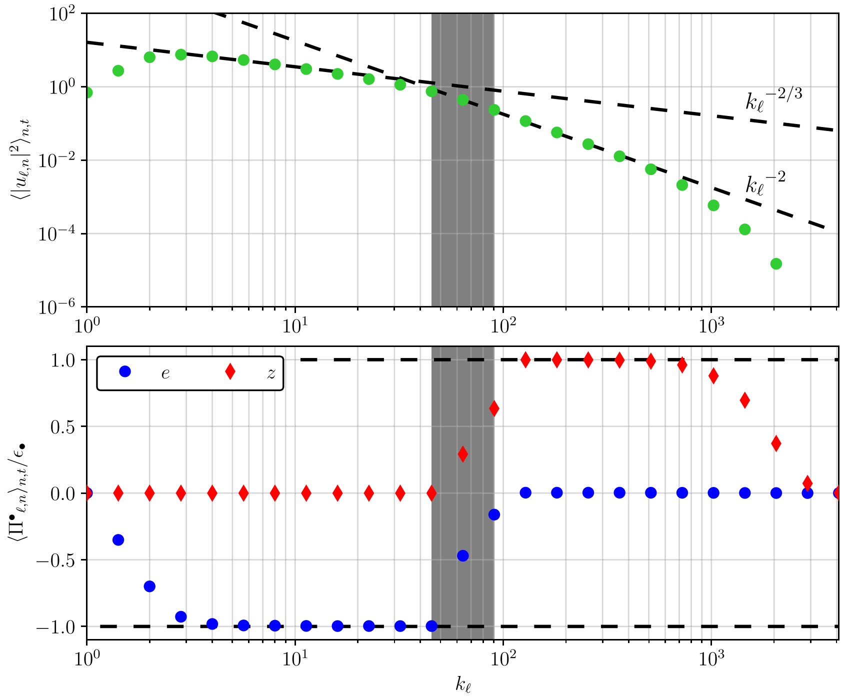

FIG. 3. Top: mean energy spectrum. The forcing band is shaded in gray. At scales larger than the forcing scale, a $k_\ell^{-2/3}$ scaling consistent with an inverse energy cascade is observed, while at smaller scales the spectrum approaches a k_ℓ^{-2} scaling consistent with a direct enstrophy cascade. Bottom: mean fluxes of the quadratic invariants, energy (blue) and enstrophy (red).

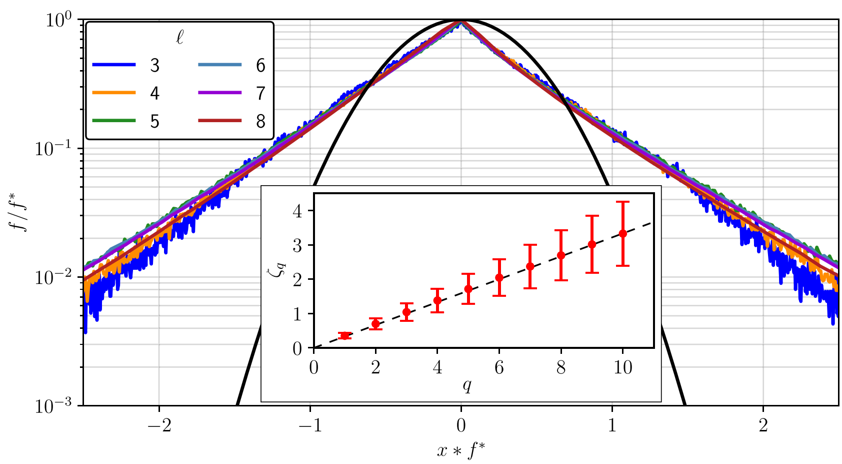

FIG. 4. Probability density functions f of the local energy flux $\Pi^{e}{}_{\ell,n}$ for ℓ within the inverse inertial range, rescaled by their maxima f^*. The Gaussian reference is shown in black. Inset: scaling exponents computed from the local energy flux structure functions; the dashed line indicates the Kolmogorov dimensional prediction.

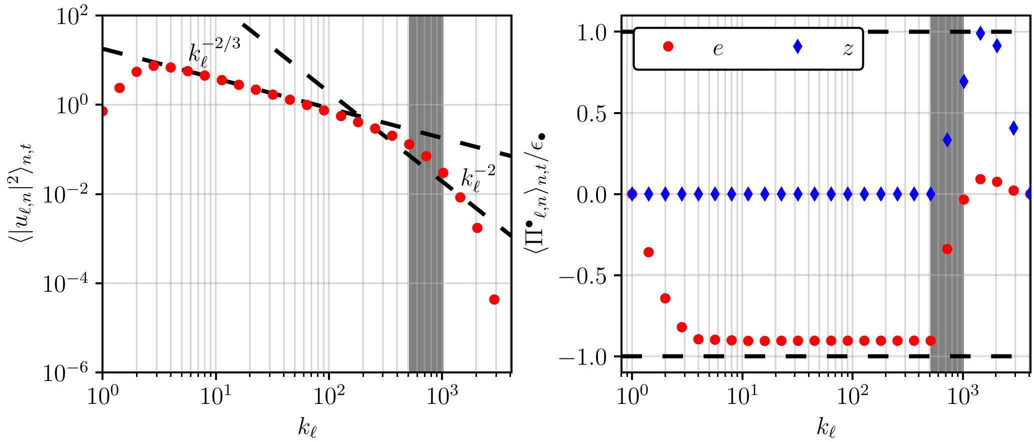

FIG. 5. Spectrum and transfers with forcing at large k.

We confirmed that the equilibrium predictions hold for this model, and we demonstrated in a shell model the emergence of a statistically stationary turbulent regime characterized by a dual cascade: an inverse cascade of energy toward large scales and a direct cascade of enstrophy toward small scales. The corresponding inertial ranges were clearly identified through the behavior of the energy spectrum and the fluxes of the two quadratic invariants.

The present setup can then be applied to model quasi-two-dimensional flows as in [6,12], however, keeping the correct dimensions of enstrophy and the correct equilibrium spectra. Another key advantage of the present framework is the possibility of defining local transfers of conserved quantities along the hierarchical structure. This allows a detailed statistical analysis of the cascade process. In particular, we observe self-similar behavior of the local energy flux together with strongly non-Gaussian fluctuations, consistent with observations in direct numerical simulations of two-dimensional Navier-Stokes turbulence.

The examined model therefore provides a minimal framework in which geometry, equilibrium properties, and cascade dynamics are consistent with the archetypal phenomenology, offering a promising tool for the theoretical investigation of systems displaying an inverse energy cascade, such as geophysical fluids.

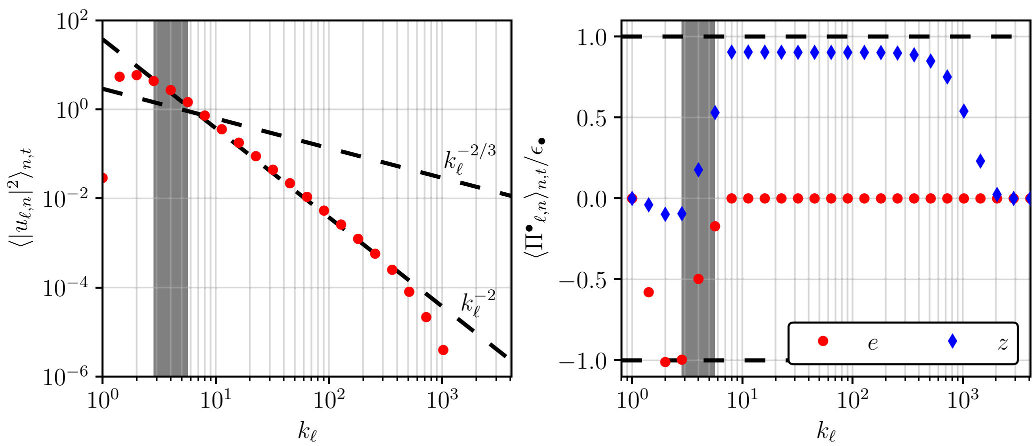

FIG. 6. Spectrum and transfers with forcing at small k.

ACKNOWLEDGMENTS

This work received financial support from the CNRS through the MITI interdisciplinary initiatives, under its exploratory research program. S.C. acknowledges funding from the ANR grant SCALP (Grant No. ANR-24-CE23-1320).

DATA AVAILABILITY

The data that support the findings of this article are not publicly available upon publication because it is not technically feasible and/or the cost of preparing, depositing, and hosting the data would be prohibitive within the terms of this research project. The data are available from the authors upon reasonable request.

APPENDIX: METHODS

We propose a parallel decomposition of the tree domain as an efficient strategy for integrating the multi-branch shell model in a parallel computational architecture. For the dyadic case, we choose a cutoff level ℓ_{cut} and distribute the variables over $2^{\ell_{\text{cut}}} + 1$ Message Passing Interface (MPI) ranks. One rank stores the upper part of the tree, namely, all nodes with $\ell < \ell_{\text{cut}}$. Each of the remaining $2^{\ell_{\text{cut}}}$ ranks stores one node at level ℓ_{cut} together with all its descendants. This decomposition is well adapted to the genealogical structure of the nonlinear coupling. Indeed, all interactions are local along branches, except for the exchange of a small number of boundary variables between the rank containing the upper tree and the ranks containing the subtrees. At each time step, the communication therefore involves only the values needed to evaluate the triads crossing the level ℓ_{cut}. This computational structure differs from that of standard pseudospectral simulations of the two-dimensional Navier-Stokes equations. In the latter case, the nonlinear term is evaluated through Fourier transforms and, in parallel implementations, usually requires global data transpositions. In the present model there is no Fourier transform and no all-to-all communication. The communication pattern is instead tree local, making the algorithm naturally scalable and well suited to accelerator-based implementations. However, the total number of degrees of freedom has the same dimensional scaling as a two-dimensional Navier-Stokes discretization. For $D = 2$, the number of variables grows as

$$N_{\text{tot}} \sim {k_{\max}}^2.$$

The advantage of the present formulation is therefore not a different memory scaling but the reduced computational complexity of the time integration. This is particularly useful for inverse-cascade problems, where long integration times are required to reach a statistically stationary state at the largest scales.

[1] T. Bohr, M. H. Jensen, G. Paladin, and A. Vulpiani, *Dynamical Systems Approach to Turbulence* (Cambridge University Press, Cambridge, UK, 1998).

[2] A. A. Mailybaev, Hidden scale invariance of turbulence in a shell model: From forcing to dissipation scales, Phys. Rev. Fluids **8**, 054605 (2023).

[3] S. Aumaître and S. Fauve, Intermittency as a consequence of a stationarity constraint on the energy flux, Phys. Rev. Lett. **132**, 114002 (2024).

[4] L. Biferale, Shell models of energy cascade in turbulence, Annu. Rev. Fluid Mech. **35**, 441 (2003).

[5] P. D. Ditlevsen, *Turbulence and Shell Models* (Cambridge University Press, Cambridge, 2010).

[6] G. Boffetta and R. E. Ecke, Two-dimensional turbulence, Annu. Rev. Fluid Mech. **44**, 427 (2012).

[7] R. H. Kraichnan, Statistical dynamics of two-dimensional flow, J. Fluid Mech. **67**, 155 (1975).

[8] R. H. Kraichnan and D. Montgomery, Two-dimensional turbulence, Rep. Prog. Phys. **43**, 547 (1980).
[9] A. Alexakis and L. Biferale, Cascades and transitions in turbulent flows, Phys. Rep. **767–769**, 1 (2018).
[10] T. Gilbert, V. S. L'vov, A. Pomyalov, and I. Procaccia, Inverse cascade regime in shell models of two-dimensional turbulence, Phys. Rev. Lett. **89**, 074501 (2002).
[11] G. Boffetta, F. De Lillo, and S. Musacchio, Shell model for quasi-two-dimensional turbulence, Phys. Rev. E **83**, 066302 (2011).
[12] S. Chen, X. M. de Wit, M. Fruchart, F. Toschi, and V. Vitelli, Odd viscosity suppresses intermittency in direct turbulent cascades, Phys. Rev. Lett. **133**, 144002 (2024).
[13] S. J. Benavides and M. D. Bustamante, Phase dynamics and their role determining energy flux in hydrodynamic shell models, Phys. Rev. Fluids **11**, 044601 (2025).
[14] E. Aurell, P. Frick, and V. Shaidurov, Hierarchical tree-model of 2D turbulence, Physica D **72**, 95 (1994).
[15] V. Zimin and F. Hussain, Wavelet based model for small-scale turbulence, Phys. Fluids **7**, 2925 (1995).
[16] E. Aurell, E. Dormy, and P. Frick, Binary tree models of high-Reynolds-number turbulence, Phys. Rev. E **56**, 1692 (1997).
[17] R. Benzi, L. Biferale, R. Tripiccione, and E. Trovatore, (1+1)-dimensional turbulence, Phys. Fluids **9**, 2355 (1997).
[18] B. Ajzner and A. Alexakis, Exact intermittent solutions in a turbulence multi-branch shell model, Atmosphere **14**, 1316 (2023).
[19] F. Tuteri, S. Chibbaro, and A. Alexakis, Ensemble of fixed points in multi-branch shell models of turbulent cascades, Physica D, **490**, 135177 (2026).
[20] M. Yamada and K. Ohkitani, Lyapunov spectrum of a model of two-dimensional turbulence, J. Phys. Soc. Jpn. **56**, 4210 (1987).
[21] V. S. Lvov, E. Podivilov, A. Pomyalov, I. Procaccia, and D. Vandembroucq, Improved shell model of turbulence, Phys. Rev. E **58**, 1811 (1998).
[22] Z. Xiao, M. Wan, S. Chen, and G. L. Eyink, Physical mechanism of the inverse energy cascade of two-dimensional turbulence: A numerical investigation, J. Fluid Mech. **619**, 1 (2009).
[23] G. Boffetta, A. Celani, and M. Vergassola, Inverse energy cascade in two-dimensional turbulence: Deviations from Gaussian behavior, Phys. Rev. E **61**, R29 (2000).
[24] X. M. de Wit, G. Ortali, A. Corbetta, A. A. Mailybaev, L. Biferale, and F. Toschi, Extreme statistics and extreme events in dynamical models of turbulence, Phys. Rev. E **109**, 055106 (2024).